



## INVESTIGATION OF CATIONIC SURFACTANTS ADSORPTION BEHAVIOUR ON SILICON WAFERS USING IMAGING ELLIPSOMETRY

Mihail Georgiev, Boris Konstantinov, Krastanka Marinova\*, Jordan Petkov, Krassimir Danov

Department of Chemical and Pharmaceutical Engineering, Faculty of Chemistry and Pharmacy, Sofia University, Sofia 1164, Bulgaria

### ARTICLE INFO

#### Article history:

Received 9 May 2023

Accepted 14 June 2023

#### Keywords:

Imaging Ellipsometry, Cationic surfactants, Adsorption layer structure, Solid surface

### ABSTRACT

The research paper explores the adsorption properties of cationic surfactants on silicon wafers through imaging ellipsometry. The objective of this research is to shed light on the layer structures formed by cationic surfactants, specifically those based on dimethyl ammonium chloride, on silicon wafers. The study involved the deposition of three distinct cationic surfactants on the wafer's surface, followed by the measurement of the adsorption layers formed. The findings reveal the creation of thin, smooth, and irregular adsorption layers. Interestingly, no correlation was found between the thickness of the adsorption layer and the surfactant tail's chain length. The research underlines the significant role which the imaging ellipsometry can have for studying surfactants' adsorption properties on surfaces, contributing to their optimal usage in various fields.

© 2023 Journal of the Technical University of Gabrovo. All rights reserved.

## 1. INTRODUCTION

Surfactants are widely used in many industries as they can modify the surface properties of materials, such as wetting, adhesion, and lubrication [1, 2, 3]. Among these, cationic surfactants have been particularly useful as bacteriocides in various applications, including the food industry and medical devices [4]. Their effectiveness as bacteriocides is directly related to their adsorption behaviour on surfaces, which boosts the interaction between the surfactant and the bacteria. Understanding the adsorption behaviour of cationic surfactants on surfaces is crucial for optimising their use as bacteriocides [5, 6].

In this paper, we present a detailed investigation of the adsorption behaviour of cationic surfactants on silicon wafers using imaging ellipsometry. This advanced ellipsometry device enables measurements of thin films and surfaces with good spatial resolution. Instead of using a single measurement spot, imaging ellipsometry scans a focused beam of light across the sample and collects data at each point (pixel) to build a two-dimensional image. This allows for detailed characterisation of variations in film thickness, refractive index, and other optical properties across the sample surface [7]. Imaging ellipsometry can be used to study a wide range of materials and systems, including thin polymer films, biological tissues, and nanomaterials.

This study aims to provide insights into the layer structure of cationic surfactants based on dimethyl ammonium chloride on silicon wafers by using imaging ellipsometry to investigate the adsorption behaviour. We

deposit three different cationic surfactants onto the silicon wafer surface and measure the resulting adsorption layers.

Using imaging ellipsometry we have demonstrated the formation of a thin, smooth, nonuniform adsorption layer of cationic surfactants without direct correlation between the surfactant tail length and the adsorption layer's thickness. Well-defined stratification layers during the evaporation of the solution on the surface has been observed in one of the systems.

In conclusion, it has been demonstrated that imaging ellipsometry is a powerful tool for characterising the adsorption behaviour of cationic surfactants on silicon wafers, which can be further used to optimise their use in various applications.

## 2. MATERIALS

Three cationic surfactants were employed, namely CatS-2C8 (Dioctyl dimethyl ammonium chloride), CatS-2C10 (Didecyl dimethyl ammonium chloride), and CatS-C8C10 (a combination of Dioctyl dimethyl ammonium chloride, Didecyl dimethyl ammonium chloride, and Decyl Octyl dimethyl ammonium chloride, as shown in Fig. 1). The solutions were prepared using deionised water generated by the Elix 5 purification system (Millipore, USA).

## 3. METHOD AND EXPERIMENTAL PROCEDURE

Ellipsometry is an optical method employed to determine the ratio of the complex-amplitude reflection coefficients of *p*- and *s*- polarised lights reflected from a surface. The ellipsometric parameters  $\Psi$  and  $\Delta$ , as shown

\* Corresponding author. E-mail: [km@lcpe.uni-sofia.bg](mailto:km@lcpe.uni-sofia.bg)

in equation (1), describe this ratio. After measuring these two parameters, a surface's refractive index and thickness can be determined using a well-established physical model [8].

$$\rho = \frac{r_P}{r_S} = \tan(\psi) e^{-i\Delta} \quad (1)$$

It is sensitive to single- and multi-layer ultrathin films, ranging from mono-atomic or monomolecular layers up to thicknesses of several microns. To determine the full dynamic range of ellipsometric parameters ( $0 \leq \psi \leq \pi/2$ ,  $0 \leq \Delta \leq 2\pi$ ) for characterising the surface of a thin film, a rotation compensator method (RCE) is used (see Fig.2). Also, this option allows us very quickly to build a 3D map of the surface where each pixel has its own  $\Psi$  and  $\Delta$ . And subject to an appropriate physical model, these values are calculated in terms of layer thickness.

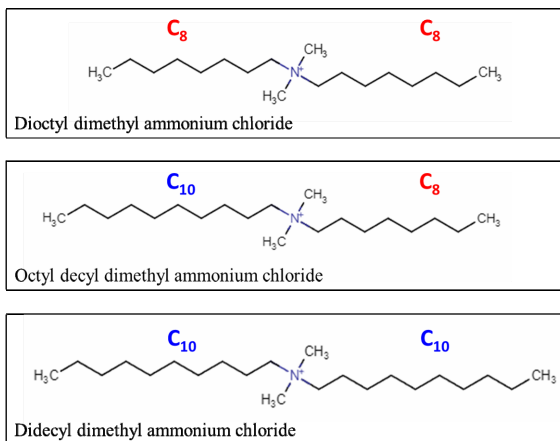


Fig. 1. Structural formulas of the used cationic surfactants

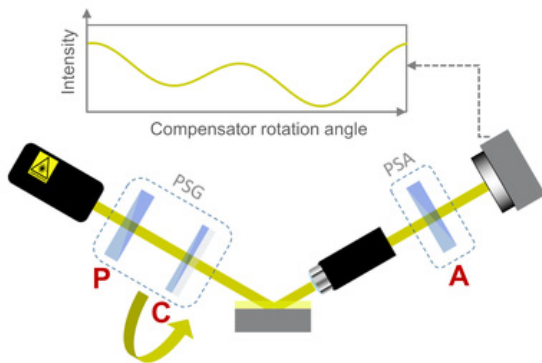


Fig. 2. Principle of rotating compensator configuration used in imaging ellipsometry

To accomplish this task, we used a NanoFilmEP4 imaging ellipsometry system (Accurion GmbH, Göttingen) equipped with a focus scanner (10x magnification). The used substrate was Si/SiO<sub>2</sub>, with a thickness of the SiO<sub>2</sub> layer equal to 234 nm. Fig. 3 displays the experimental results for the determined thickness.

$$n(\lambda) = A + \frac{B}{\lambda^2} + \frac{C}{\lambda^4} \quad (2)$$

The analysis of the optical parameters  $\Psi$  and  $\Delta$  in terms of deposited layer thickness requires the determination of the refractive index of the layer. In this study, the deposited surfactant layer is characterized by the

Cauchy equation (eq. 2) for a transparent layer, which is an empirical relationship between the refractive index,  $n$ , and the wave length,  $\lambda$ .

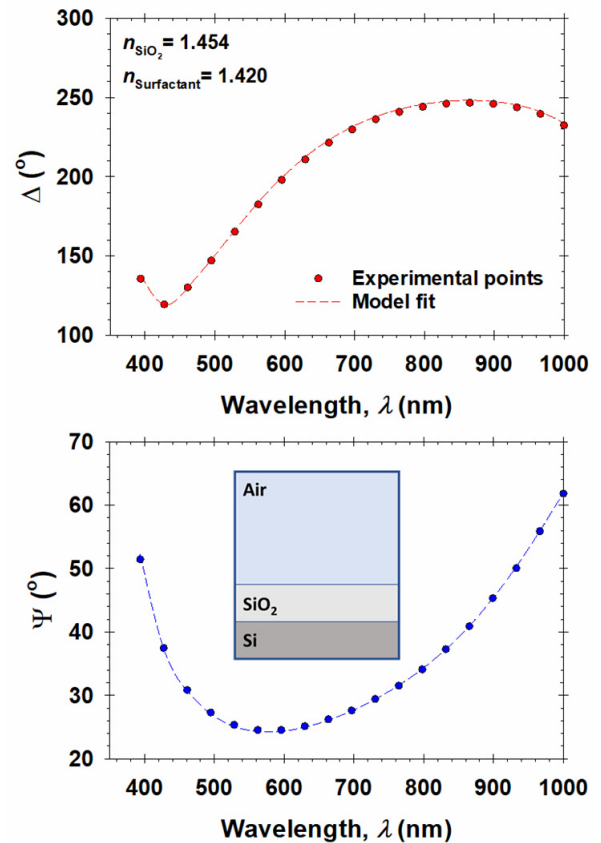


Fig. 3. Measured  $\Delta$  and  $\Psi$  values as a function of the wavelength at an angle of incidence = 60° for the bare Si/SiO<sub>2</sub> surface. The experimental points are taken at an ellipsometric nulling condition in four-zone measurement to use the maximum accuracy of the technique. The picture represents an illustration of the physical model used to calculate the thickness of the SiO<sub>2</sub> layer

The mathematical model that fits the objective physical reality quite well includes a substrate of Si, above it an atomically smooth layer of SiO<sub>2</sub> on which there is a molecularly smooth layer of surfactant, and the environment is air, as shown in the picture in Fig. 3. Defining the thickness of the SiO<sub>2</sub> allows us to upgrade the model with an additional layer, those of the adsorbed surfactant, and continue to use the one-layer ellipsometry task. This means that all deviations in the  $\Delta$  and  $\Psi$  will be attributed to the thickness of the surfactant layer. A refractive index value of 1.42 was used for all calculations pertaining to the surfactant layer.

The treatment protocol involves using kimwipes soaked in a 1 ml solution to perform five circular wiping on a bare silicon wafer. Following the wiping, the surface is coated with small droplets of the solution, which quickly evaporate.

#### 4. RESULTS AND DISCUSSION

##### Adsorption layer from CatS-C8C10

In Fig. 4A, the results of imaging ellipsometry are presented, displaying the surfactant layer remaining on the surface of a silicon wafer after treatment with a solution of CatS-C8C10 at a concentration of 0.5 wt%. Notably, the layer that forms from surfactant evaporation increases in

thickness from the top to the bottom of the wafer. The residual droplet area is visible as a yellow region in the image and is observable to the naked eye, as shown in Fig. 5A. Dense stratification layers form around these residual droplets, and the thickness of the layer increases towards the center of the droplet due to increasing concentration from solution evaporation. The first layer measured has a thickness of 3.3 nm, and the first five layers exhibit a slope of 3.24 nm, indicating they are a stack of lamellar sheets. Linear regression is observed even after the fifth layer, although with a different slope equal to 2.14 nm (see Fig. 4C). Possible explanations for this observation suggest that the first five layers are formed mainly by Didecyl surfactant molecules due to their higher surface activity than Dioctyl surfactants. Due to their shorter chain length, Dioctyl monomers may form the upper layers with a thinner step. Alternatively, the upper layer may contain a mixture of Didecyl and Dioctyl monomers, based on possible tilting in the chains of the upper layers due to the exhaustion of larger chain-length surfactants for the formation of the first five layers.

#### Adsorption layer from CatS-2C8

The images presented in Fig. 5, obtained using imaging ellipsometry, show the surface topography of a silicon wafer treated with a 0.5 wt% solution of CatS-2C8. The first image (Fig. 5A) displays a section with a smooth and dense layer on the surface with a thickness of approximately 5 nm. The next two images (Fig. 5B and 5C) reveal additional steps with a thickness of 5 nm each. The final layer, depicted in Fig. 5C, consists of spherical aggregates with a thickness of roughly 20 nm. Notably, these aggregates are not visible to the naked eye but leave a visibly greasy surface, as shown in Fig. 7B. Collectively, these images provide insight into the surface structure of the silicon wafer after treatment with CatS-2C8 and suggest the presence of a spread adsorption layer.

#### Adsorption layer from CatS-2C10

In Figure 6, the imaging ellipsometry results illustrate the adsorption characteristics of CatS-2C10, the surfactant featuring two decyl tails per monomer. Away from the droplet evaporation regions, the adsorption layer appears to be non-dense, exhibiting a thickness of 2.5 nm, as evident from Figure 6A. In contrast, closer to the evaporated droplets, we observe a disordered formation of thick adsorption layers, displaying thicknesses above 40 nm, as evident from Figures 6B and 6C.

#### Optical properties of the treated surface

When the silicon wafer is treated with the surfactant solution, the evaporation of the residual tiny droplets leaves visible spots on it.

Representative images of the treated surface are illustrated in Fig. 7. From the pictures, we can generally distinguish two regions: (i) transparent region, where the surface is optically clear, and (ii) oily regions, where even with the naked eye we can distinguish the surfactant adsorption layers and the spots resulting from the evaporation. Actually, for all the investigated surfactants, the ellipsometry measurements of the optically clear transparent region show the presence of a thin adsorption

layer. For the surfactant with two C8 chains (CatS-2C8), the thickness of this transparent layer is 5 nm, whereas, for the surfactant with two C10 chain lengths, this thickness is 2.5 nm.

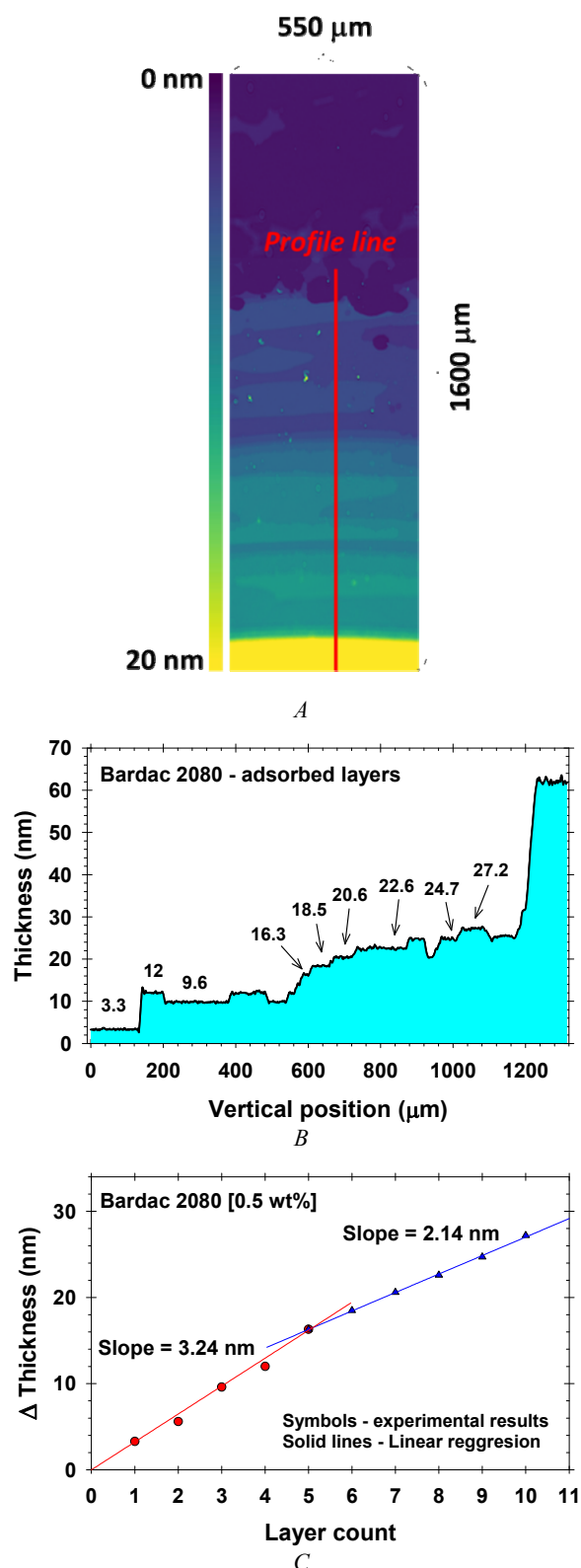


Fig. 4. Experimental results of 0.5% CatS-C8C10. A) Images obtained using imaging ellipsometry; B) Thickness of the adsorbed layer at the red profile line shown in A; C) arrangement of the sequence of thickness taken from the profile by their value

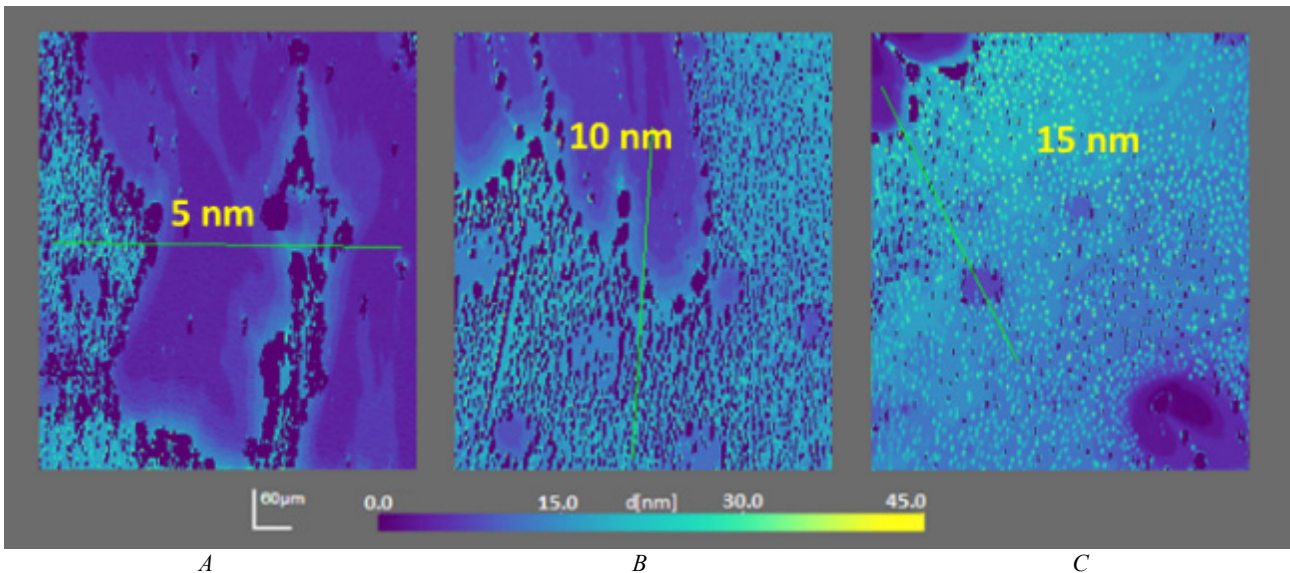


Fig. 5. Images obtained using imaging ellipsometry, which displays the surface topography of a silicon wafer after treatment with a solution of CatS-2C8 with a concentration of 0.5 wt%. All the images are representative of the most frequently observed structure

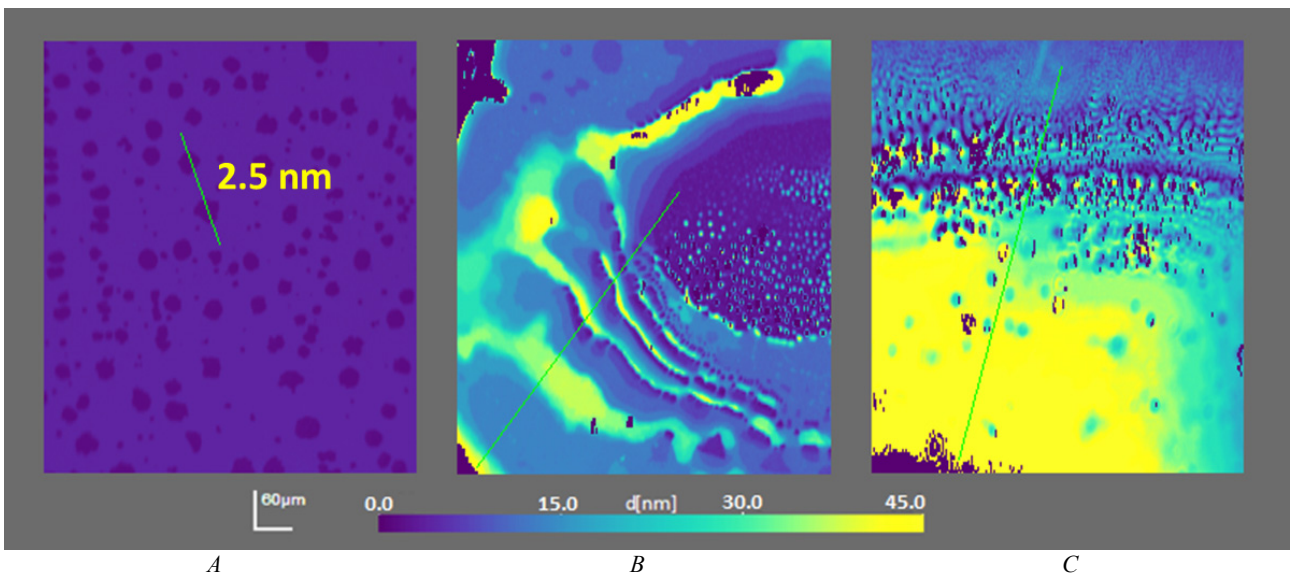


Fig. 6. Images obtained using imaging ellipsometry, which displays the surface topography of a silicon wafer after treatment with a solution of CatS-2C10 with a concentration of 0.5 wt%. All the images are representative of the most frequently observed structure

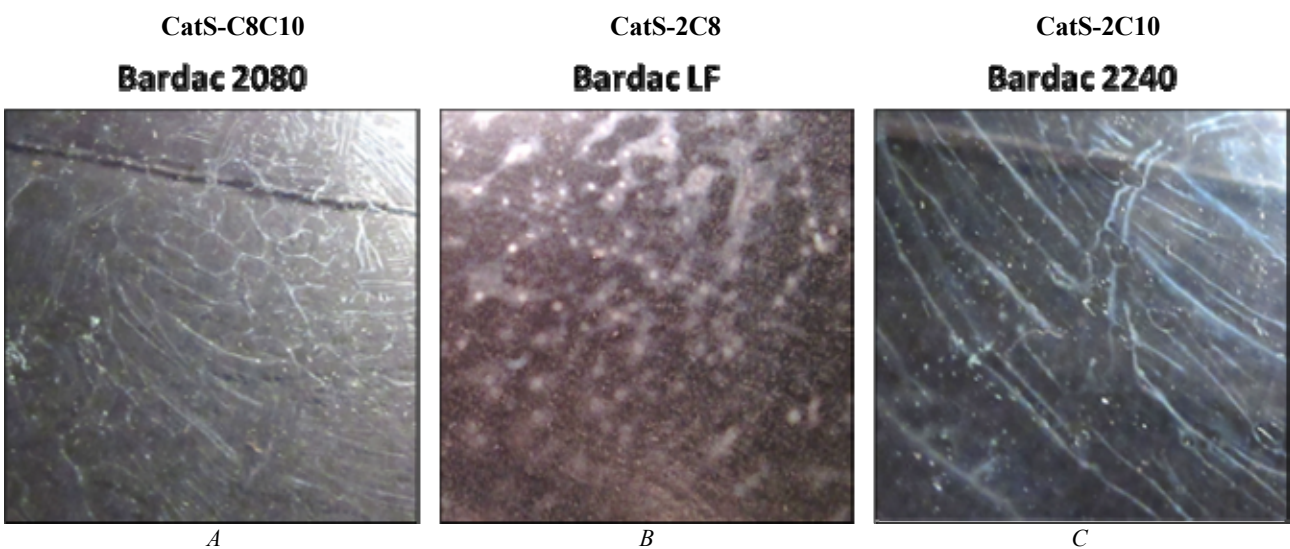


Fig. 7. Images of the silicon wafer surface treated with the different cationic surfactants, including A) CatS-C8C10; B) CatS-2C8; and C) CatS-2C10, where the scale bar is 1 cm

## 5. CONCLUSIONS

The adsorption layers formed by three different surfactants (CatS-C8C10, CatS-2C8, and CatS-2C10) on a silicon wafer using imaging ellipsometry have been studied. The thickness and structure of these layers vary depending on the surfactant used. CatS-C8C10 forms a layer that increases in thickness from the top to the bottom of the wafer, with the first five layers being a stack of lamellar sheets. CatS-2C8 forms a dense and smooth layer approximately 5 nm thick, with spherical aggregates in the last layer. CatS-2C10 forms a non-dense adsorption layer away from droplet evaporation regions, while thick and disordered layers form close to these regions. The optical properties of the treated surface are also analysed, with a thin adsorption layer present in the transparent area for all three surfactants. Overall, the study provides valuable insights into the adsorption behaviour of these surfactants on silicon wafers, which could have significant implications in various industries and applications.

## ACKNOWLEDGEMENTS

*The authors gratefully acknowledge the support from the Operational Programme "Science and Education for Smart Growth", Bulgaria, project No.BG05M2OP001-1.002-0023*

## REFERENCES

- [1] Farias C., Almeida F., Silva I. et al./Electronic Journal of Biotechnology 51 (2021) 28–39
- [2] Nedyalkov M. et al./Colloids and Surfaces A: Physicochem. Eng. Aspects 354 (2010) 22–27
- [3] Lim M., Stokes J./Biotribology 28 (2021) 100199
- [4] Khan M. et al./Colloids and Surfaces B: Biointerfaces 132 (2015) 216–224
- [5] Atkin R. et al./Advances in Colloid and Interface Science 103 (2003) 219–304
- [6] Kékicheff P., Contal C./Langmuir 35 (8) (2019) 3087-3107
- [7] Azzam R., Bashara N., Ellipsometry and Polarized Light (1988)
- [8] C.-J. Yu et al./Microelectronics Reliability 55 (2015) 352–357